Scaling law for coherent vortices in decaying drift Rossby wave turbulence

Watanabe, Takeshi
Iwayama, Takahiro
Fujisaka, Hirokazu

Scaling law for coherent vortices in decaying drift Rossby wave turbulence

Takeshi Watanabe,[1,*] Takahiro Iwayama,[2] and Hirokazu Fujisaka[1]
[1]*Department of Physics, Kyushu University 33, Fukuoka 812-81, Japan*
[2]*Department of Control Engineering and Science, Faculty of Computer Science and Systems Engineering, Kyushu Institute of Technology, Iizuka 820, Japan*
(Received 11 June 1997; revised manuscript received 29 September 1997)

We numerically study the time evolution of coherent vortices in decaying turbulence described by the Charney-Hasegawa-Mima equation with the weak dissipation. Self-organized coherent vortices develop through the mutual advection and the vortex merging. The dimensional analysis provides the dynamical scaling law of structure function of the potential vorticity field $S(k,t)=E^{5/4}\lambda^{1/2}t^{1/2}G(k/\overline{k(t)})$ [$\overline{k(t)}\sim E^{-1/8}\lambda^{3/4}t^{-1/4}$] with a scaling function $G(x)$, which turns out to be in good agreement with numerical experiments. In physical space, quantities related to coherent vortices develop algebraically with time. The dimensional analysis predicts that the total number N of vortices decreases as $N\sim t^{-\chi}$ with exponent $\chi=1/2$. Moreover, it is found that the remarkable feature of this system is the approximate conservation of the area of the coherent region in the potential vorticity field. [S1063-651X(98)01802-9]

PACS number(s): 47.27.Eq, 47.32.Cc, 52.35.Ra, 92.60.Ek

I. INTRODUCTION

Two-dimensional (2D) turbulence has been extensively studied theoretically and numerically since the 1960s because the large-scale motion of the atmosphere and the ocean or the magnetofluid under the uniform, strong magnetic field are described approximately by the two-dimensional fluid dynamics. In addition, it is easier to carry out the numerical experiments for 2D turbulence than for 3D turbulence.

Through the direct numerical simulation (DNS) of 2D turbulence, the existence of the ordered structure of the turbulent field in physical space has attracted researchers' interest. According to numerical studies on the 2D turbulence in recent years [1–3], it has been found that the remarkable feature of this system is the existence of coherent vortices in physical space, which dominates the dynamics of the turbulent field.

The role of coherent vortices in 2D turbulence has been studied in detail through the study of 2D decaying Navier-Stokes (NS) turbulence. In the time evolution, the so-called second stage in which coherent vortices dominate the dynamics of the system, coherent vortices cause mutual advection, which is approximately described by Hamiltonian dynamics of the 2D point vortex system. Furthermore, when vortices with the same sign of circulation are within a critical distance, they merge into larger vortices. A phenomenological scaling theory to the evolution of vortex statistics is proposed in [4–6] and the validity of the scaling theory is confirmed by both the DNS of the 2D NS equation and the numerical simulation of the point vortex model. Moreover, a scaling exponent ξ characterizing the scaling theory is phenomenologically determined in [7].

Recently, the 2D turbulence described by the Charney-Hasegawa-Mima (CHM) equation has been actively studied theoretically and numerically. This equation approximately describes the time evolution of the flow in the geostrophic equilibrium in the planetary atmosphere and is called the quasigeostrophic potential vorticity equation [8]. Furthermore, the time evolution of the quasi-2D fluctuation of the electrostatic field on the plane perpendicular to the strong magnetic field uniformly applied to plasma is also described by this equation [9]. The CHM equation in the strong turbulent state neglecting the effect of wave is written as

$$\frac{\partial q}{\partial t}+J(\phi,q)=0, \tag{1}$$

where $\mathbf{r}=(x,y)$, $\nabla=(\partial/\partial x,\partial/\partial y)$, $J(a,b)=a_xb_y-a_yb_x$, and $q(\mathbf{r},t)=(\nabla^2-\lambda^2)\phi(\mathbf{r},t)$ denotes the potential vorticity. Here $\phi(\mathbf{r},t)$ denotes the geostrophic stream function in the geophysical case or the electrostatic potential in plasma. The parameter λ is the characteristic wave number expressing the ratio of the system size to the Rossby radius in the atmosphere or the ion Larmor radius in plasma. Equation (1) resembles the vorticity equation derived from the 2D Euler equation, which is in fact identical to Eq. (1) in the limit $\lambda\to 0$. In the case of $\lambda\neq 0$, the CHM equation includes a characteristic spatial scale λ^{-1} and ϕ corresponding to the stream function of the 2D NS equation can be represented as

$$\phi(\mathbf{r},t)=-\frac{1}{2\pi}\int K_0(\lambda|\mathbf{r}-\mathbf{r}'|)q(\mathbf{r}',t)\,d\mathbf{r}', \tag{2}$$

where $K_0(z)$ is the modified Bessel function of the second kind. That is, the stream function at the position $\mathbf{r}$ affected by the potential vorticity at the position $\mathbf{r}'$ is limited within the range of $O(\lambda^{-1})$. This fact shows that the CHM equation indicates unique behavior differing from the 2D NS equation.

In this system, several works have been carried out for the freely decaying and the forced turbulence. In the freely decaying turbulence, the dependence of the statistical properties in the turbulent field on the parameter λ is numerically investigated in detail [10]. In the forced turbulence, it is reported that the crystal-like structure of the vortices, which is

*Electronic address: nabe3scp@mbox.nc.kyushu-u.ac.jp

called ''vortical quasicrystalization'' [11,12], is formed after full time evolution. Then the dynamical properties of the vortices in this formation process are studied in detail in [12] and the dynamical scaling law is derived from the consideration of the energy inverse cascade process. Furthermore, the study of the dynamics of the coherent structure in the CHM system is carried out for the forced and decaying turbulence [13] and the relation between the suppression of the energy inverse cascade and the coherent structure is discussed.

In this paper we study the dynamics of coherent vortices in the region characterizing the drift Rossby wave turbulence, i.e., $\lambda \gg k$, by using the DNS of the CHM equation with weak dissipation from the statistical point of view. Since the characteristics of coherent vortices appear remarkably in the decaying turbulence rather than the forced turbulence, we especially investigate the decaying turbulence.

This paper is organized as follows. Briefly explaining the DNS of the CHM equation and presenting its results in Sec. II, we discuss the dynamical properties of the structure function of the potential vorticity q in the wave-number space in Sec. III. In Secs. IV and V we discuss the characteristics of coherent vortices in the physical space and derive the dynamical scaling law for coherent vortices, respectively. In Sec. VI we discuss and summarize our results.

II. DIRECT NUMERICAL SIMULATION

To investigate the emergence of coherent vortices and its dynamics in the CHM turbulence, we numerically solve Eq. (1) with the dissipation term $(-1)^{p+1}\nu\nabla^{2p}(\nabla^2\phi)$, $p=2$, by using the pseudospectral method [14]. The system size L, the parameter λ, and a hyperviscosity coefficient ν are fixed as $L=2\pi$, $\lambda=40$, and $\nu=3.0\times10^{-8}$, respectively. The physical space resolution is set to 256×256 with the maximum wave number $k_c=85$. The numerical integration is performed for 40 000 time steps by using the fourth-order Runge-Kutta method with the time increment $\Delta t=2.5\times10^{-3}$ in double precision.

An initial condition is used by generating Gaussian random numbers with the mean value 0 and the variance 1 for phase of each Fourier component of ϕ. Moreover, we normalize the initial value of the total energy per unit area

$$E=\frac{1}{L^2}\int_0^L\int_0^L\frac{1}{2}[(\nabla\phi)^2+\lambda^2\phi^2]dx\,dy=\int_0^{k_c}E(k)\,dk \tag{3}$$

to be 0.5, where $E(k)$ is the energy spectrum. The initial form of $E(k)$ in wave-number space is specified as

$$E(k)\sim\frac{k^{30}}{(k+k_0)^{60}}. \tag{4}$$

This form is the same initial condition as used in [10], which is the very narrow wave-number band spectrum at the center k_0. We choose $k_0=50$ to set $k_0>\lambda$. In this case, it is found that the initial energy of the system is almost concentrated on the wave-number region of $k>\lambda$. This initial condition is appropriate for investigating how the structure of coherent vortices develops from small-scale vortices.

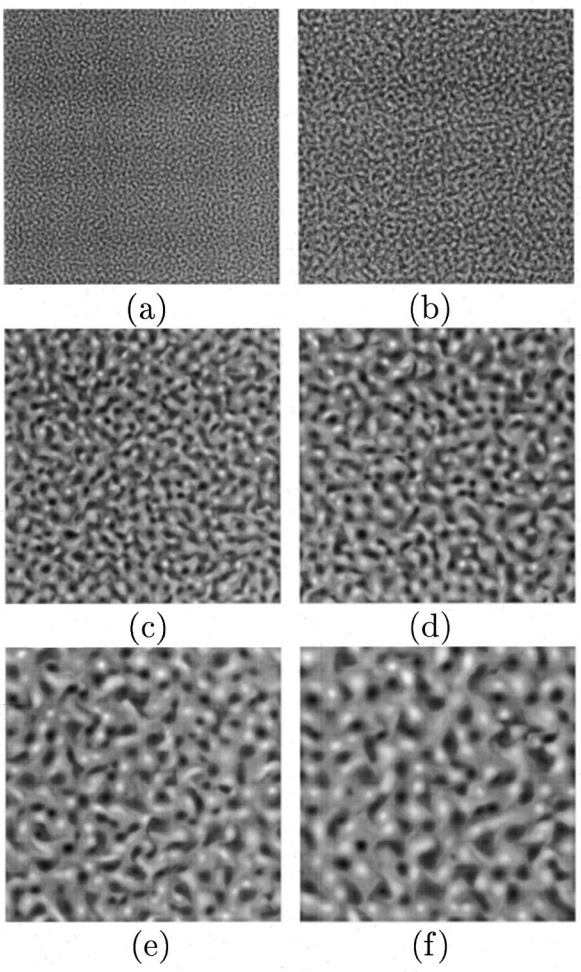

FIG. 1. Snapshots of the potential vorticity field $q=\nabla^2\phi-\lambda^2\phi$ at (a) $t=0$, (b) $t=1$, (c) $t=10$, (d) $t=20$, (e) $t=50$, and (f) $t=100$. The white (black) region indicates $q>0$ $(q<0)$.

A typical time evolution of the potential vorticity field $q(\mathbf{r},t)$ is shown in Fig. 1. One observes that the potential vorticity field self-organizes into a set of coherent vortices from the random initial condition. These coherent vortices develop into larger spatial size and their total number decreases gradually with time. These observations originate from the fact that the vortices with the same sign of circulation within a critical distance merge through the mutual advection and become larger vortices in the turbulent field. Figure 1 shows that coherent vortices hardly move and form a quasi-steady-state as a set of the monopole structure of the potential vorticity q in a sufficient long time. This state extensively differs from the second stage of the 2D decaying NS turbulence which is specified by both the active mutual advection and the vortex merging. The time development of the energy spectrum corresponding to this process is shown in Fig. 2. We can confirm that the peak position of the energy spectrum that is initially set to $k=50$ moves temporally toward the small-wave-number side and its moving rate in the region of $k<\lambda$ slows down gradually. The asymptotic form of the energy spectrum is approximately $E(k)\sim k^{-6}$, whose slope is a little steeper than the result derived in Sec. II of [12], $E(k)\sim k^{-5}$. This result is almost consistent with the energy spectrum given in [10]. The difference between the power law of the energy spectrum in the potential enstro-

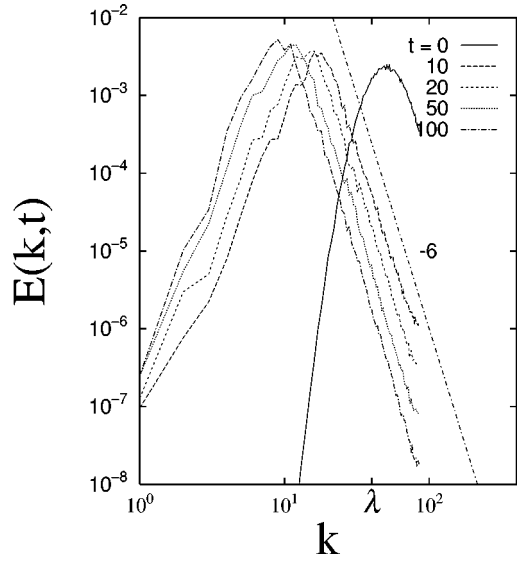

FIG. 2. Time evolution of the energy spectrum $E(k,t)$. λ is set to be 40 in our simulation.

phy cascade region derived from the dimensional analysis and that obtained by the numerical simulation is reminiscent of the difference between the $E(k)\sim k^{-3}$ and k^{-4} as known in 2D decaying NS turbulence [2], but the consideration of the cause of the difference is beyond the scope of this paper.

III. STRUCTURE FUNCTION OF POTENTIAL VORTICITY FIELD AND DYNAMICAL SCALING LAW

In order to examine the dynamical properties of the potential vorticity field q in wave-number space, we observe the structure function $S(k,t)$ of q at each time step,

$$S(k,t)=\left\langle \left| \int q(\mathbf{r},t)e^{-i\mathbf{k}\cdot\mathbf{r}}\, d\mathbf{r} \right|^2 \right\rangle, \tag{5}$$

where $\langle\ \rangle$ represents the average taken over the orientation of $\mathbf{k}$. If the structure function has a sharp single peak, a characteristic wave number $\overline{k(t)}$ exists in the potential vorticity field, which gives a mean distance $l_a(t)=2\pi/\overline{k(t)}$ among centers of neighboring coherent vortices with the same sign of circulation. According to the time evolution of $\overline{k(t)}$, we can thus discuss the dynamical property of the characteristic spatial scale. The quantity $\overline{k(t)}$ is defined by using the structure function $S(k,t)$ as

$$\overline{k(t)}=\frac{\Sigma_{k=0}^{\lambda} kS(k,t)}{\Sigma_{k=0}^{\lambda} S(k,t)}. \tag{6}$$

Since the wave-number region of main interest is $k\ll\lambda$, the upper limit of the wave number in Eq. (6) is set at λ. Moreover, we also pay attention to the time evolution of the peak height $S_{\max}(t)$ of the structure function. We can expect that the mean distance l_a among vortices with same sign of circulation [characteristic wave number $\overline{k(t)}$] increases [decreases] with time because the total number N of coherent vortices will decrease with time by merging vortices.

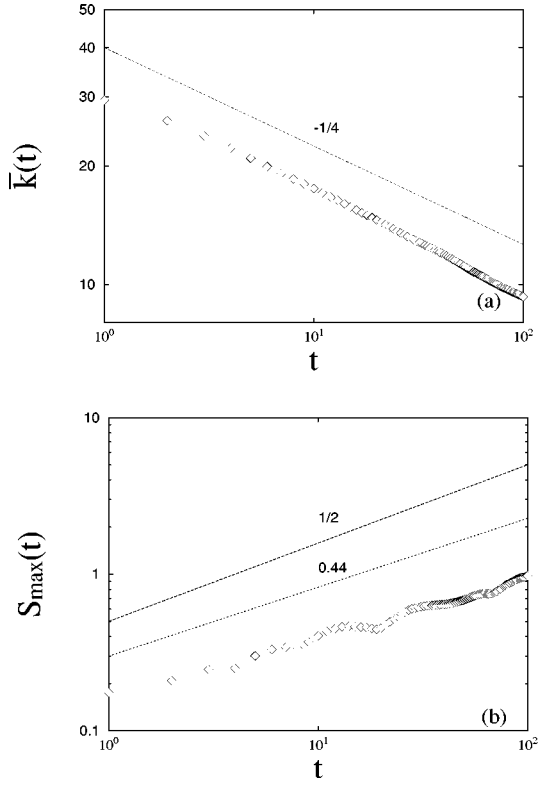

FIG. 3. Time evolution of (a) the characteristic wave number $\overline{k(t)}$ and (b) the peak height $S_{\max}(t)$ of the structure function $S(k,t)$. The slopes $-1/4$ and $1/2$ are theoretical values, respectively, and the reasonable value 0.44 may be due to the effect of finite Reynolds number.

Numerical results of the time evolution of $\overline{k(t)}$ and $S_{\max}(t)$ are shown in Fig. 3. As is expected, $\overline{k(t)}$ algebraically decreases with time, while $S_{\max}(t)$ increases with time. This phenomenon is expected to be closely connected with the energy inverse cascade process. We find that the time evolution of $\overline{k(t)}$ and $S_{\max}(t)$ obeys the power law of time t, which is evaluated from Fig. 3 as $\overline{k(t)}\sim t^{-0.2}$ and $S_{\max}(t)\sim t^{0.4}$.

By using the results of the dynamical scaling law derived in [12] for the developing process in CHM turbulence, the scaling law of $\overline{k(t)}$ and $S_{\max}(t)$ is derived as follows. The assumption that the energy transfer rate $\epsilon\sim E/t$ is constant with time was introduced to derive the dynamical scaling law in [12]. In decaying CHM turbulence with high Reynolds number, on the other hand, the total energy E can be approximately regarded as the conserved quantity after a full time evolution. Therefore, the substitution of $\epsilon\sim E/t$ into the dynamical scaling laws [Eqs. (17) and (20) in [12]] by assuming that E is constant yields the modified dynamical scaling law as

$$\overline{k(t)}\sim E^{-1/8}\lambda^{3/4}t^{-1/4}, \tag{7}$$

$$S_{\max}(t)\sim E^{5/4}\lambda^{1/2}t^{1/2}. \tag{8}$$

The scaling law $\overline{k(t)}\sim t^{-1/4}$ turns out to be in good agreement with the result shown in Fig. 3, while $S_{\max}(t)\sim t^{1/2}$

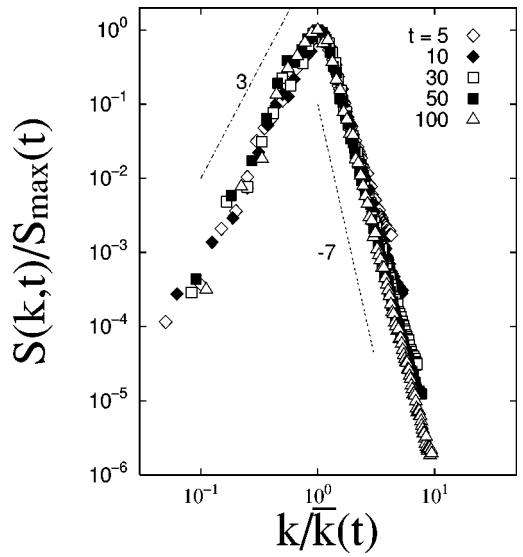

FIG. 4. Scaling plots of $S(k,t)/S_{\max}(t)$ vs $k/\overline{k}(t)$ at $t=5$, 10, 30, 50, and 100.

seems to be overestimated. This discrepancy between the dimensional analysis and the numerical result will be discussed later.

Furthermore, in order to examine how to evolve $S(k,t)$ with time, $S(k,t)/S_{\max}(t)$ vs $k/\overline{k}(t)$ is plotted for different times in Fig. 4. This figure clearly indicates that the structure function of q satisfies the dynamical scaling law

$$\frac{S(k,t)}{S_{\max}(t)} = G\left(\frac{k}{\overline{k}(t)}\right), \tag{9}$$

where $G(x)$ is a universal scaling function. The asymptotic form of the scaling function $G(x)$ is found to be

$$G(x) \sim \begin{cases} x^{-\gamma}, & x>1 \\ x^{\delta}, & x<1, \end{cases} \tag{10}$$

where the scaling exponents are $\gamma \approx 7$ and $\delta \approx 3$ from Fig. 4.

In [12] we numerically found that the dynamical scaling law is valid in the wave-number region smaller than λ in the developing process of forced CHM turbulence and derived the scaling exponents of both $\overline{k}(t)$ and $S_{\max}(t)$ theoretically. In this paper we also find the dynamical scaling law in decaying turbulence similar to that in forced turbulence. However, the value of the scaling exponents and the asymptotic form of the scaling function are different from each other.

A scaling law the same as Eq. (7) has been derived in [10] under the assumption that the energy spectrum develops, maintaining a similar form temporally. We observed that the structure function of the potential vorticity field obeys the dynamical scaling law, so we conclude that this result is consistent with that of the energy spectrum developing in a self-similar way with time.

IV. CHARACTERISTICS OF COHERENT VORTICES IN PHYSICAL SPACE

In the preceding section we discussed the statistical properties of the characteristic quantities concerning with the wave-number space by investigating the time evolution of the structure function of $q(\mathbf{r},t)$ without referring to details of the coherent structure appearing in the potential vorticity field. This is closely connected with the energy inverse cascade process which is a characteristic of the dynamics in the wave-number space of the CHM equation.

In physical space, on the other hand, coherent vortices self-organize from the random initial state, merge through the mutual advection, and develop into larger vortices. To discuss the dynamics of coherent vortices in physical space, we have to extract the region of coherent vortices from the potential vorticity field.

In order to extract the coherent region from the potential vorticity field, we define a coherent region as that where the following two conditions are satisfied simultaneously: (i) The Gaussian curvature Q of ϕ, defined as

$$Q = \left(\frac{\partial^2\phi}{\partial x \partial y}\right)^2 - \left(\frac{\partial^2\phi}{\partial x^2}\right)\left(\frac{\partial^2\phi}{\partial y^2}\right), \tag{11}$$

is negative and (ii) the absolute value of the potential vorticity $|q|$ is larger than $\langle|q|\rangle$, which is the average value of $|q|$ taken over the total area of the system, i.e., $\langle|q|\rangle = 1/L^2 \int_{L^2}|q|\, d\mathbf{r}$. The reason for the definition of the above conditions is as follows. The coherent region should have the stable structure and Q is a standard measure of the stability of the Lagrangian particle [2,6]. In addition, we expect that the coherent region has a large absolute value of the potential vorticity. We write the area of coherent region as $S_{\rm coh}$.

Figure 5 shows coherent regions defined by the above conditions at $t=10$, 100, respectively. Comparing Fig. 5 with the potential vorticity field in Fig. 1, we can recognize that the regions of the axisymmetrical vortices are extracted. The time evolution of the area of the coherent region, normalized by the total area, is shown in Fig. 6. It seems that the area is almost constant with time after forming coherent vortices and is about 25% for the initial condition used in this paper. This result indicates that the region of coherent vortices is approximately conserved with time and that is an important characteristic of coherent vortices in the CHM turbulence.

Next we consider the behavior of the energy and the potential enstrophy for coherent vortices defined above. It is shown numerically [6] that the integral values of the two expressions of the energy density $(\nabla\phi)^2/2$ and $-\phi\nabla^2\phi/2$ over the coherent region are different from each other. By inferring from the Hamiltonian dynamics of the point vortex system, the latter is the Hamiltonian for coherent vortices and is the fundamental conserved quantity in 2D decaying NS turbulence [6]. In the CHM system, it is expected from the analogy to the 2D NS system that the integral value of $-\phi q/2$ over the coherent region is the Hamiltonian for the coherent region. For coherent vortices obtained in our simulation, Fig. 7 shows the time evolutions of the total energy E, E_1, and E_2, where E_1 and E_2 are defined as

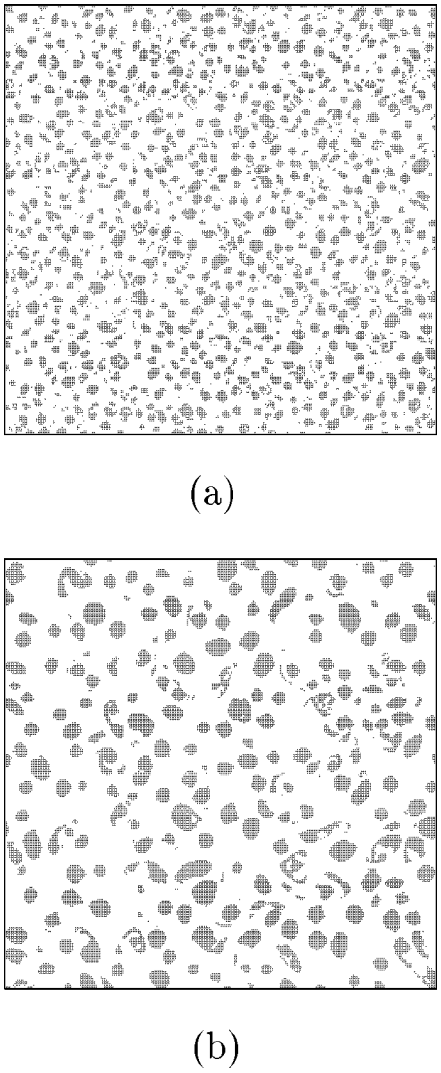

FIG. 5. Coherent regions at (a) $t=10$ and (b) $t=100$.

$$E_1=\frac{1}{L^2}\int_{S_{\rm coh}}\left(-\frac{1}{2}\phi q\right)\,d\mathbf{r}$$

$$=\frac{1}{L^2}\int_{S_{\rm coh}}\frac{1}{2}[-\phi\nabla^2\phi+\lambda^2\phi^2]\,d\mathbf{r}, \qquad (12)$$

$$E_2=\frac{1}{L^2}\int_{S_{\rm coh}}\frac{1}{2}[(\nabla\phi)^2+\lambda^2\phi^2]\,d\mathbf{r}. \qquad (13)$$

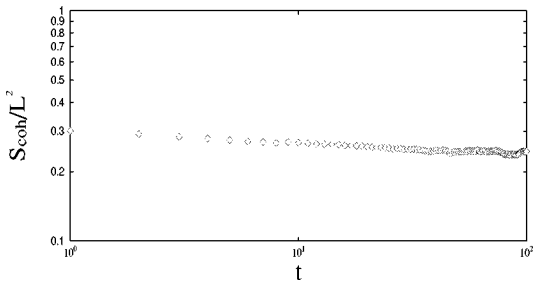

FIG. 6. Time evolution of the ratio of the area $S_{\rm coh}$ of the coherent region to the total area L^2.

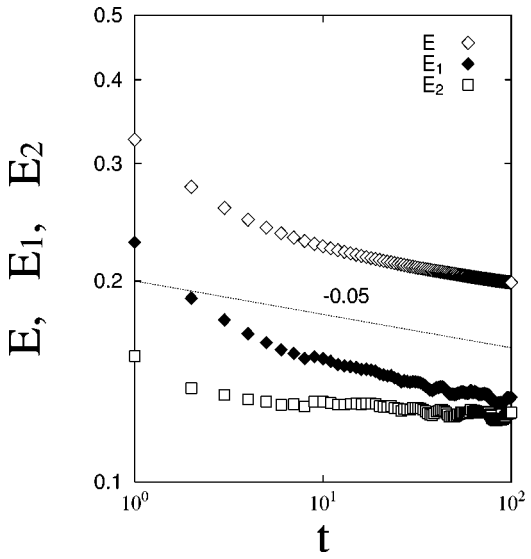

FIG. 7. Time evolution of E, E_1, and E_2 defined in Sec. IV. A slope of -0.05 indicates that the energy slightly decreases with time due to the finite Reynolds number effect.

Note that if integrands in Eqs. (12) and (13) are integrated over the total area, they coincide with E. The quantities E_1 and E_2 temporally evolve in a different way. However, the difference between E_1 and E_2 decreases with time and they approach an almost constant value. This result originates from the difference between the integral values of $-\phi\nabla^2\phi/2$ and $(\nabla\phi)^2/2$ in Eqs. (12) and (13). However, for $\lambda\gg k$, these quantities are very small in comparison to the integral value of $\lambda^2\phi^2/2$ over the coherent region. Therefore, E_1 and E_2 remain almost the same after the full time evolution ($E_1/E=0.67$ and $E_2/E=0.64$ at $t=100$). By taking into consideration that the behaviors of the time evolution of E and E_1 are almost the same and E_1 occupies most of E, E_1 can be regarded as a characteristic energy for coherent vortices. In other words, since the energy E_1 concerning the coherent region is clearly a large portion of E in the whole time region in spite of the area of the coherent region being small, $S_{\rm coh}/L^2=0.25$–0.3, the system behavior is dominated by the dynamics of the coherent vortices. As will be seen later, the difference between $-\phi\nabla^2\phi/2$ and $(\nabla\phi)^2/2$ remarkably appears in the time evolution of the potential enstrophy rather than that of the energy.

Figure 8 shows the time evolution of the total potential enstrophy U, U_1, and U_2 defined as

$$U_1=\frac{1}{L^2}\int_{S_{\rm coh}}\frac{1}{2}q\nabla^2\phi\,d\mathbf{r}$$

$$=\frac{1}{L^2}\int_{S_{\rm coh}}\frac{1}{2}[(\nabla^2\phi)^2-\lambda^2\phi\nabla^2\phi]\,d\mathbf{r}, \qquad (14)$$

$$U_2=\frac{1}{L^2}\int_{S_{\rm coh}}\frac{1}{2}[(\nabla^2\phi)^2+\lambda^2(\nabla\phi)^2]\,d\mathbf{r}. \qquad (15)$$

Note that if the integrands in Eqs. (14) and (15) are integrated over the total area, they coincide with U. Figure 8 clearly shows that U_1 occupies the large amount of U

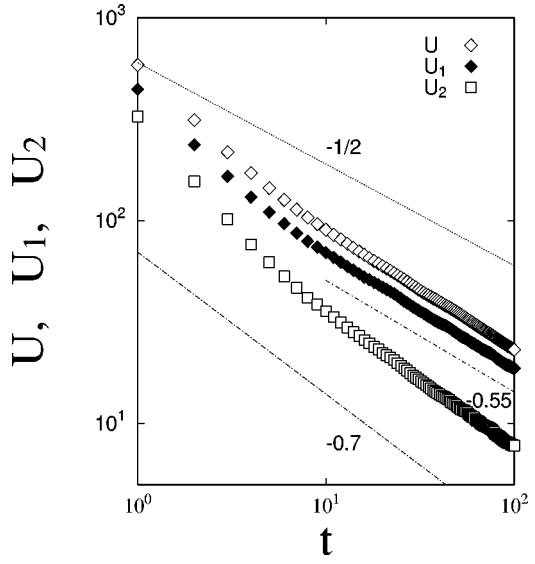

FIG. 8. Time evolution of U, U_1, and U_2 defined in Sec. IV. The slope $-1/2$ is the theoretical value derived in Sec. V and the value -0.55 may be due to the effect of finite Reynolds number.

($U_1/U=0.81$ at $t=100$) and the time evolution of U_1 indicates almost the same power law as U, which is estimated as $U_1 \sim t^{-0.5}$. On the other hand, U_2 has a very small value in comparison with U or U_1 ($U_2/U=0.33$ at $t=100$) and decreases with time faster than U or U_1 as $U_2 \sim t^{-0.7}$. These results originate from the difference between $-\lambda^2\phi\nabla^2\phi/2$ and $\lambda^2(\nabla\phi)^2/2$ in Eqs. (14) and (15). Particularly in the case of $\lambda \gg k$ the difference is remarkable. The difference is equivalent to that of the first terms of the integrands in Eqs. (12) and (13). According to the numerical results, U_1 can be regarded as a characteristic potential enstrophy for coherent vortices because U_1 has the same order of magnitude U and the same temporal behavior as that of U. E_1 and U_1 are different from E_2 and U_2 and are, as will be shown in the next section, connected with the vortex dynamics.

V. SCALING THEORY FOR PHYSICAL QUANTITIES OF COHERENT VORTICES

In this section, in analogy to the scaling theory developed in the second stage of 2D decaying NS turbulence [4], we propose a scaling theory that describes the time evolution of average quantities related to coherent vortices. Our standpoint is that coherent vortices self-organized for a random initial condition dominate the dynamics of the system and that the energy E_1 and the potential enstrophy U_1 relating to coherent vortices are therefore expressed in terms of characteristic quantities of vortices.

First, we assume that the potential enstrophy q is approximately written as

$$q=\nabla^2\phi-\lambda^2\phi\approx-\lambda^2\phi \tag{16}$$

for $k \ll \lambda$. By employing Eq. (16), E_1 and U_1 can be expressed in terms of the total number N of coherent vortices, their average radius r_a, and the average potential vorticity q_a of vortex centers as

$$E_1 \approx \frac{1}{L^2}\int_{S_{\rm coh}}\frac{1}{2}\lambda^2\phi^2\, d\mathbf{r} \sim N\lambda^{-2}q_a^2r_a^2, \tag{17}$$

$$U_1 \approx -\frac{1}{L^2}\int_{S_{\rm coh}}\frac{1}{2}\lambda^2\phi\nabla^2\phi\, d\mathbf{r} \sim N\lambda^{-2}q_a^2. \tag{18}$$

If E_1 and q_a are regarded as conserved quantities of the system in the high Reynolds number limit, Eq. (17) yields

$$Nr_a^2 \sim t^0. \tag{19}$$

Equation (19) clearly indicates that the area of the coherent region is constant with time and is consistent with the numerical results shown in Fig. 6.

If the total number of vortices N decreases algebraically with time as

$$N(t) \sim t^{-\chi}, \tag{20}$$

we can derive the scaling laws of $r_a(t)$ and $U_1(t)$ from Eqs. (18) and (19) as

$$r_a(t) \sim t^{\chi/2}, \tag{21}$$

$$U_1(t) \sim t^{-\chi}. \tag{22}$$

Moreover, the average distance l_a between vortices with same sign of circulation is evaluated as

$$l_a(t) \sim \frac{1}{\sqrt{N(t)}} \sim t^{\chi/2}. \tag{23}$$

Namely, the exponents of dynamical scaling of the quantities related to vortices are expressed only by χ.

In Sec. III, we found that the time evolution of the characteristic wave number $\overline{k(t)}$ corresponding to the peak position of the structure function of q obeys the scaling $\overline{k(t)} \sim E^{-1/8}\lambda^{3/4}t^{-1/4}$ [Eq. (7)]. Since the inverse of $\overline{k(t)}$ is regarded as the average distance among vortices with the same sign of circulation, which corresponds to l_a, Eq. (7) yields the scaling law for l_a,

$$l_a(t) \sim \frac{1}{\overline{k(t)}} \sim t^{1/4}. \tag{24}$$

By combining Eqs. (23) and (24), the scaling exponent is determined as

$$\chi=\frac{1}{2}. \tag{25}$$

Consequently, the dynamical scaling of the other quantities related to the vortices are evaluated as

$$N(t) \sim t^{-1/2}, \quad r_a(t) \sim t^{1/4}, \quad U_1(t) \sim t^{-1/2}. \tag{26}$$

In the numerical simulation, the power law of $U_1(t)$ can be easily compared with the above result. As shown in Fig. 8, the scaling $U_1(t) \sim t^{-1/2}$ is in agreement with the numerical

result, although the theoretical exponent is somewhat smaller than the experimental value. This deviation will be discussed in Sec. VI.

Here we discuss the implication that r_a and l_a have the same scaling exponents. In physical space, coherent vortices with the same sign of circulation develop into larger ones through the vortex merging, conserving the area of the coherent region. The fact that the growing laws of $r_a(t)$ and $l_a(t)$ are the same in this coagulation process indicates that the potential vorticity field q temporally develops in a self-similar way. This is the reason for the existence of the dynamical scaling law [Eq. (9)]. On the other hand, in the scaling theory for coherent vortices in 2D decaying NS turbulence [4–7], the scaling laws of $r_a(t)$ and $l_a(t)$ are represented as

$$r_a(t) \sim t^{\xi/4}, \quad l_a(t) \sim t^{\xi/2}, \tag{27}$$

where ξ is the scaling exponent of the total number of the vortices $N \sim t^{-\xi}$. Equation (27) implies that coherent vortices gradually become thin as time passes because the growth rate of $l_a(t)$ is larger than that of $r_a(t)$.

VI. SUMMARY AND DISCUSSION

We investigated the statistical characteristic of the structure function of q in wave-number space for $\lambda \gg k$ and the dynamical properties of coherent vortices in physical space in decaying CHM turbulence. We developed the scaling theory for the time evolution of the quantities related to the vortices in analogy to that in 2D decaying NS turbulence. Our analytical results are in good agreement with the results obtained from DNS.

An important result obtained in this study is that the area of the coherent region is conserved with time, $Nr_a^2 \sim t^0$, even in the time region where the vortices actively merge. It was clarified in Sec. V that this result is one of the intrinsic characteristics of the dynamics of coherent vortices with scale larger than the characteristic scale $2\pi/\lambda$. This should be compared with the fact that in the second stage of 2D decaying NS turbulence, Nr_a^4 is conserved with time and that the area of the coherent region is not conserved. This difference seems to be important when we discuss the dynamics of coherent vortices by using the point vortex dynamics for CHM turbulence [15,16].

Finally, we discuss the effect of the finite Reynolds number on the scaling exponents evaluated from the scaling theory. The scaling theory of the energy spectrum in wave-number space and that of quantities related to coherent vortices in physical space are valid in the limit of infinite Reynolds number. The energy is not conserved completely and slightly decreases with time on account of the effect of viscosity. From Fig. 7 we suppose that the temporal decrease of E and E_1 behaves as

$$E, E_1 \sim t^{-\theta}, \tag{28}$$

although the area of the coherent region is conserved. Substituting Eq. (28) into Eqs. (7) and (8), we obtain the correction of the scaling law as

$$\overline{k(t)} \sim \lambda^{3/4} t^{-(2-\theta)/8}, \tag{29}$$

$$S_{\max}(t) \sim \lambda^{1/2} t^{(2-5\theta)/4}. \tag{30}$$

Moreover, by substituting $q_a^2 \sim t^{-\theta}$, which is the result from $E_1 \sim t^{-\theta}$ and $Nr_a^2 \sim t^0$, into Eq. (18) yields

$$U_1(t) \sim t^{-(1+2\theta)/2}. \tag{31}$$

If we estimate $\theta \approx 0.05$ from Fig. 7, Eqs. (29)–(31) are evaluated as

$$\overline{k(t)} \sim t^{-0.24}, \quad S_{\max}(t) \sim t^{0.44}, \quad U_1(t) \sim t^{-0.55}. \tag{32}$$

As shown in Figs. 3 and 8, the correction of the scaling exponents for $S_{\max}(t)$ and $U_1(t)$ are in good agreement with the results of our simulation. The extent of correction of a scaling exponent for $\overline{k(t)}$ is about 2.5% in comparison to the original one, i.e., the scaling exponent does not change much. Consequently, it seems that the correction of the scaling exponents for N or r_a is small.

APPENDIX: DETERMINATION OF THE SCALING EXPONENT χ FROM THE HAMILTONIAN DYNAMICAL ADVECTION SCALING

We discuss the derivation of the scaling exponent χ from the consideration of the Hamiltonian dynamical advection of vortices. According to Ref. [7], the velocity of the vortex center is evaluated as

$$u_a \sim \frac{H}{\Gamma_a l_a}, \tag{A1}$$

where Γ_a is the average circulation. In 2D decaying NS turbulence, the Hamiltonian $H \sim Nr_a^4 \omega_a^2$ and ω_a are conserved. By using $u_a \sim t^{-\xi}$, ξ being defined as $N \sim t^{-\xi}$, derived from Eqs. (27) and (A1), $u_a \sim dl_a/dt$, we obtain the scaling exponent $\xi = 2/3$. However, in the case of the CHM equation, as mentioned in the present paper, we have obtained that Nr_a^2 must be conserved compared to Nr_a^4 for the Hamiltonian H. Therefore, if we assume that E_1 is a Hamiltonian H in CHM turbulence, H is expressed as $H \sim Nr_a^2 \lambda^{-2} q_a^2$ from Eq. (17). Substituting $\Gamma_a \sim t^{\chi}$ and $l_a \sim t^{\chi/2}$ obtained from Eq. (20) into Eq. (A1) leads to the scaling law

$$u_a \sim t^{-3\chi/2}. \tag{A2}$$

This result indicates that the advection velocities of vortices slows down with time. Moreover, if we assume that the advection velocity is evaluated as the time variation of the distance among vortices (the relative velocities of vortices),

$$u_a \sim \frac{dl_a}{dt} \sim \frac{l_a}{t}, \tag{A3}$$

then from Eqs. (23), (A2), and (A3) the scaling exponent is derived as

$$\chi = \frac{1}{2}. \tag{A4}$$

This agrees with the value [Eq. (25)] obtained in the scaling theory of the energy inverse cascade in wave-number space.

[1] J. C. McWilliams, J. Fluid Mech. **146**, 21 (1984).
[2] R. Benzi, S. Patarnello, and P. Santangelo, J. Phys. A **21**, 1221 (1988).
[3] J. C. McWilliams, Phys. Fluids A **2**, 547 (1990).
[4] G. C. Carnevale, J. C. McWilliams, Y. Pomeau, J. B. Weiss, and W. R. Young, Phys. Rev. Lett. **66**, 2735 (1991).
[5] J. B. Weiss and J. C. McWilliams, Phys. Fluids A **5**, 608 (1993).
[6] T. Iwayama and H. Okamoto, Prog. Theor. Phys. **96**, 1061 (1996).
[7] T. Iwayama, H. Fujisaka, and H. Okamoto Prog. Theor. Phys. (to be published).
[8] J. Pedlosky, *Geophysical Fluid Dynamics* (Springer-Verlag, New York, 1987).
[9] A. Hasegawa and K. Mima, Phys. Fluids **21**, 87 (1978).
[10] V. D. Larichev and J. C. McWilliams, Phys. Fluids A **3**, 938 (1991).
[11] N. Kukharkin, S. A. Orszag, and V. Yakhot, Phys. Rev. Lett. **75**, 2486 (1995).
[12] T. Watanabe, H. Fujisaka, and T. Iwayama, Phys. Rev. E **55**, 5575 (1997).
[13] C. Ferro Fontan and A. Verga, Phys. Rev. E **52**, 6717 (1995).
[14] S. A. Orszag, Stud. Appl. Math. **100**, 293 (1971).
[15] M. Kono and W. Horton, Phys. Fluids B **3**, 3255 (1991).
[16] N. J. Zabusky and J. C. McWilliams, Phys. Fluids **25**, 2175 (1982).